Theoret. Chim. Acta (Berl.) 48, 349–356 (1978)

THEORETICA CHIMICA ACTA

Interpretation of Soft X-Ray Emission Spectra in Terms of Relativistic Electric Dipole Transition Probabilities

Applications to VC and NbC

Peter Weinberger

Institut für Technische Elektrochemie, Technische Universität Wien, Getreidemarkt 9, A-1060 Wien, Austria

Franz Rosicky

Institut für Theoretische Chemie und Strahlenchemie, Universität Wien, Währingerstrasse 17, A-1090 Wien, Austria

The emission process for eigenstates of a model Dirac Hamiltonian of "muffin-tin" type is described in terms of relativistic electric dipole (E1) transitions with the assumption that the final state is a localized core eigenstate of the system. The proposed method is applied to the L-emission spectrum of V in VC and to the L- and M-emission spectrum of Nb in NbC. Resulting theoretical spectra are compared with experimental data.

Key words: X-ray emission spectra, soft, of V and Nb

1. Introduction

In the present paper the emission process for eigenstates of a model Dirac Hamiltonian of "muffin-tin"-type is described in terms of relativistic electric dipole transitions with the assumption that the final state is a (localized) core eigenstate of the system. The non-relativistic counterpart of this approach has been applied to Blochfunctions [1] and discussed in terms of local solid state models [2].

2. Theoretical Approach

The probability per unit time for a transition from an initial state $|i\rangle$ to a final state $|f\rangle$, caused by an interaction operator H' is, in first order time dependent perturbation theory, proportional to $\Delta E \cdot S|\langle i|H'|f\rangle|^2$, where $\Delta E = E_f - E_i$ and S denotes an average and summation over all appropriate unobservables. In the present investigations H' is (in the radiation gauge) given by $H' = \boldsymbol{\alpha}\boldsymbol{A}$, where $\boldsymbol{\alpha}$ are the three skew symmetric Dirac matrices and $\boldsymbol{A}$ is the vector potential of the radiation field.

The most general expressions for atomic relativistic electromagnetic multipole transition probabilities were originally obtained by Rosner and Bhalla [3]. In the

0040-5744/78/0048/0349/$01.60

present paper this problem is simplified by considering only the electric dipole transitions in the extreme long-wavelength limit. Thus

$$A^{(e)}_{1,M} \sim \xi_M, \tag{1}$$

where the polarization basis vectors are given by

$$\xi_{M=\pm 1} = \mp \frac{1}{\sqrt{2}}(e_1 \pm i e_2) \tag{2}$$

$$\xi_{M=0} = e_3 .$$

In the following the theory of multipole fields is applied as presented by Rose [4].

Using the commutator relation $\alpha = i/\hbar c[H_0^D, x]$, where H_0^D denotes the unperturbed Dirac Hamiltonian and using the calculus of irreducible spherical tensors, then

$$\Delta E \cdot S |\langle i|\alpha A^{(e)}_{1,M}|f\rangle|^2 \sim (\Delta E)^3 \cdot S |\langle i|r Y_1^M|f\rangle|^2 = D_{if} . \tag{3}$$

For a particular central-field region of the "muffin-tin"-potential the final state $|f\rangle$ (core state) is an eigenbispinor of H_0^D for a definite energy E, total angular momentum j and parity P:

$$|f\rangle = |E_f, Q_f\rangle = \begin{Bmatrix} G(E_f, \kappa_f|r)|\kappa_f \mu_f\rangle \\ iF(E_f, \kappa_f|r)|-\kappa_f \mu_f\rangle \end{Bmatrix}, \tag{4}$$

where $Q=(\kappa\mu)$, $j=|\kappa|-\frac{1}{2}$, $-j \leqslant \mu \leqslant j$, $P=(-1)^{j+a/2}$, $a=\kappa/|\kappa|$ and $\kappa = \mp 1, \mp 2, \mp 3, \ldots$ The initial state $|i\rangle$ (valence state) can be constructed in terms of a linear combination of partial waves

$$|i\rangle = \sum_{Q_i} C_{Q_i}(E_i)|E_i, Q_i\rangle, \tag{5}$$

where the summation is restricted by the selection of rules for the electric dipole transitions and $C_{Q_i}(E_i)$ are normalized expansion coefficients to be obtained from e.g. the relativistic SW-theory [5, 6], the relativistic KKR-method [7, 8], the relativistic OPW-method [9] or the relativistic APW-method [10]. In the following the pairs of indices Q_f and Q_i will be denoted by $Q=(\kappa\mu)$ and $Q'=(\kappa'\mu')$, respectively.

The use of the Wigner–Eckart theorem yields

$$\sqrt{\frac{4\pi}{3}}\langle \kappa\mu| Y_1^M|\kappa'\mu'\rangle = (-1)^{\mu+1/2}[(2j+1)(2j'+1)]^{1/2} \cdot \begin{pmatrix} j & 1 & j' \\ -\mu & M & \mu' \end{pmatrix}\begin{pmatrix} j & 1 & j' \\ \frac{1}{2} & 0 & -\frac{1}{2} \end{pmatrix}. \tag{6}$$

Since S denotes $4\pi/3 \sum_M \sum_\mu$, then utilizing the orthogonality relations of the Wigner 3-j-symbols

$$D_{if} = \frac{4\pi}{3}(\Delta E)^3 \sum_{Q'} |C_{Q'}(E_i)|^2 (2j+1) \begin{pmatrix} j & 1 & j' \\ \frac{1}{2} & 0 & -\frac{1}{2} \end{pmatrix}^2 R^2_{\kappa\kappa'}(E_f, E_i), \tag{7}$$

where

$$R_{\kappa\kappa'}(E_f, E_i) = \int_0^R r^3[G(E_f, \kappa \mid r)G(E_i, \kappa' \mid r) + F(E_f, \kappa \mid r)F(E_i, \kappa' \mid r)]dr \quad (8)$$

and R is the atomic sphere radius. Using the definition of κ-like charges $Q_\kappa(E)$

$$Q_\kappa(E) = N_\kappa(E) \sum_\mu |C_Q(E)|^2,$$

where

$$N_\kappa(E) = \int_0^R r^2[G^2(E, \kappa \mid r) + F^2(E, \kappa \mid r)]dr \quad (10)$$

(7) can be formulated as

$$D_{if} = (\Delta E)^3(2j+1) \sum_{\kappa'} \begin{pmatrix} j & 1 & j' \\ \frac{1}{2} & 0 & -\frac{1}{2} \end{pmatrix}^2 R^2_{\kappa\kappa'}(E_f, E_i) N^{-1}_{\kappa'}(E_i) Q_{\kappa'}(E_i).$$

Finally summing over all occupied initial states $|i\rangle$ the relative intensity $I(E)$ is given by

$$I(E) \sim \sum_i \delta(E_i - E_f - h\nu) D_{if}$$

$$= (\Delta E)^3 \delta(E - E_f - h\nu)(2j+1) \sum_{\kappa'} \begin{pmatrix} j & 1 & j' \\ \frac{1}{2} & 0 & -\frac{1}{2} \end{pmatrix}^2 R^2_{\kappa\kappa'}(E_f, E) N^{-1}_{\kappa'}(E) \chi_{\kappa'}(E), \quad (11)$$

where $\chi_\kappa(E)$ is the κ-like local density of states

$$\chi_\kappa(E) = \sum_i Q_\kappa(E_i) \delta(E - E_i). \quad (12)$$

3. Applications

It was found that relativistic effects in the valence region are negligibly small for VC and rather small for NbC [11]. This suggests to approximate the energy distribution functions $\chi_\kappa(E)$ by their non-relativistic counterparts, i.e. to approximate the κ-like charges $Q_\kappa(E_i)$ by $\bar{Q}_\kappa(E_i)$

$$\bar{Q}_\kappa(E_i) = \frac{(2j+1)}{2(2l+1)} Q_l(E_i). \quad (14)$$

In Table 1 a comparison of $Q_\kappa(E_i)$ and $\bar{Q}_\kappa(E_i)$ is shown for typical metal "d"- and Carbon "p"-valence states. Since the differences between $Q_\kappa(E_i)$ and $\bar{Q}_\kappa(E_i)$ are small, (12) is applied in the following way

$$I(E) \sim (\Delta E)^3 \delta(E - E_f - h\nu) \sum_{\kappa'} T_{\kappa\kappa'}(E_f, E) \chi_l(E) \quad (15)$$

Table 1. Comparison of κ-like charges Q_κ and $\bar{Q}_\kappa$ for VC and NbC. (i refers to single space group symmetry, i' to double space group symmetry, energies are given in Rydbergs. All charges listed are multiplied by the corresponding degeneracies)

Compound	Sphere	i	E_i	i'	$E_{i'}$	κ	Q_κ	$\bar{Q}_\kappa$
VC	V	Γ_{12}	0.7814	Γ_8^+	0.7771	2	1.2744	1.3806
						−3	2.1800	2.0710
	C	Γ_{15}	0.8432	Γ_6^-	0.8404	1	1.5670	1.5684
				Γ_8^-	0.8426	−2	3.1364	3.1368
NbC	Nb	Γ_{12}	0.8833	Γ_8^+	0.8686	2	1.1068	1.2366
						−3	2.0004	1.8550
	C	Γ_{15}	0.8300	Γ_6^-	0.8232	1	1.4670	1.4698
				Γ_8^-	0.8281	−2	2.9342	2.9376

where the $T_{\kappa\kappa'}(E_f, E)$ are

$$T_{\kappa\kappa'}(E_f, E) = \frac{[2j+1][2j'+1]}{2(2l'+1)} R^2_{\kappa\kappa'}(E_f, E) N_{\kappa'}^{-1}(E) \begin{pmatrix} j & 1 & j' \\ \frac{1}{2} & 0 & -\frac{1}{2} \end{pmatrix}^2 \tag{16}$$

and $\chi_l(E)$ is the l-like local density of states for the central-field under consideration.

The l-like local density of states functions are given by Neckel *et al.* [12] for VC and by Schwarz [13] for NbC. The radial transition probabilities (16) are calculated using the corresponding self-consistent APW crystal potentials.

In Figures 1–3 the radial transition probabilities (16) are shown for the V-L, Nb-L and Nb-M emission. For Nb they are shown together with the case where the non-relativistic (NR) limit [7, 8] is applied for the valence states. For the V-L emission the radial transition probabilities differ only slightly from those obtained

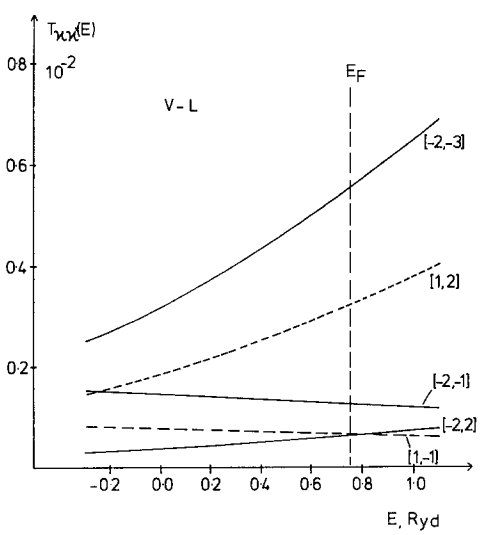

Fig. 1. Radial transition moments $T_{\kappa\kappa'}(E_f, E)$ (16) for the V-L emission in VC. In the square brackets $[\kappa, \kappa']$ κ refers to the core state

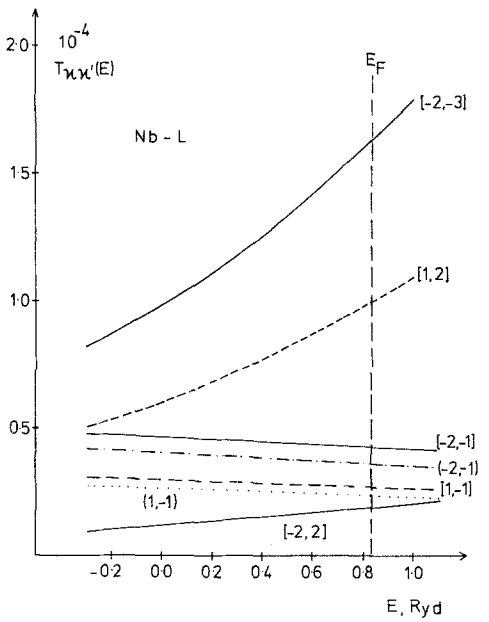

Fig. 2. Radial transition moments $T_{\kappa\kappa'}(E_f, E)$ (16) for the Nb-L emission in NbC. In the square brackets $[\kappa, \kappa']$ κ refers to the core state. Round brackets (κ, κ') indicate the cases where the non-relativistic limit is applied for the valence states

using the NR limit for the corresponding valences states. Even for Nb corresponding emissions from an "s"-like valence state to a "$2p$" core state differ only by about 10%. In Figs. 1–3 all possible transitions, namely $\Delta j = 0 \pm 1$, are displayed. Eq. (16) automatically provides the correct intensity ratios for the theoretical L_2 and L_3, M_4 and M_5 emission spectrum, respectively.

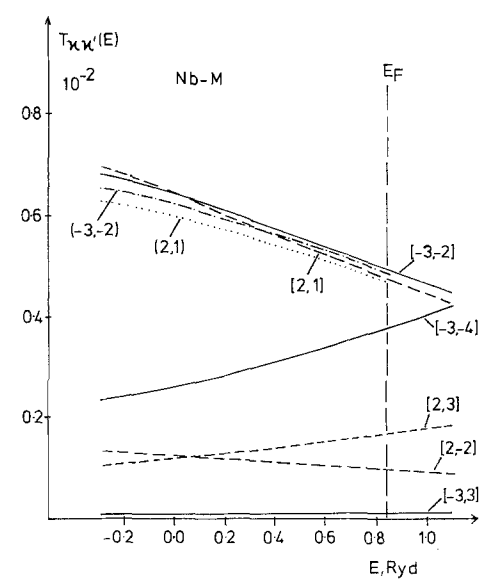

Fig. 3. Radial transition moments $T_{\kappa\kappa'}(E_f, E)$ (16) for the Nb-M emission in NbC. In the square brackets $[\kappa, \kappa']$ κ refers to the core state. Round brackets (κ, κ') indicate the cases where the non-relativistic limit is applied for the valence states

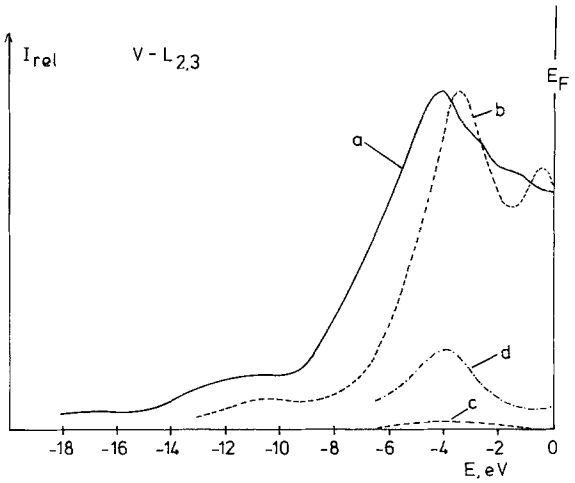

Fig. 4. The V-$L_{2,3}$ emission spectrum for VC in the energy range of the theoretical L_3 spectrum: (a) experimental spectrum [14], (b) theoretical L_3 spectrum, (c) theoretical L_2 spectrum, (d) theoretical L_2 spectrum enlarged by ten times

In Fig. 4 the experimental V-$L_{2,3}$ emission spectrum in VC [14] is compared with the theoretically calculated L_2 and L_3 spectrum, based on the parameters γ_0 (life time broadening), W (energy dependent valence broadening) and S (spectrometer resolution) [15], listed in Table 2. For VC the effects of the L_2 emission on the L_3 emission spectrum is rather small, since the corresponding core levels are separated by 6.73 eV and since the natural line widths [18] lead to a broader L_2 emission spectrum.

In Fig. 5 two experimental M spectra [16, 17] for Nb in NbC are shown with the theoretical M_4 and M_5 spectrum (Table 2). The experimental spectrum b [17] is shifted such that the highest peak coincides with the corresponding peak in spectrum a [16]. For the Nb-$M_{4,5}$ spectrum the consideration of relativistic transition probabilities is of some interest, since the $3d^{3/2}$ and $3d^{5/2}$ core levels differ only 2.75 eV in energy and consequently a separation of the experimental $M_{4,5}$ spectrum seems dubious. Spectrum b shows that the $3d^{5/2}$ emission is favoured in terms of broadening effects as compared with the $3d^{3/2}$ emission.

Table 2. Line widths (γ_0), energy dependent broadening parameters (W) and spectrometer resolutions (S) [eV]

	γ_0	W	S
V-L_2	1.42[18]	1.0	1.0
V-L_3	0.79[18]	1.0	1.0
Nb-L_2	2.09[18]	1.0	0.5
Nb-L_3	1.69[18]	1.0	0.5
Nb-M_4	1.40	0.5	0.35
Nb-M_5	0.25	0.5	0.35

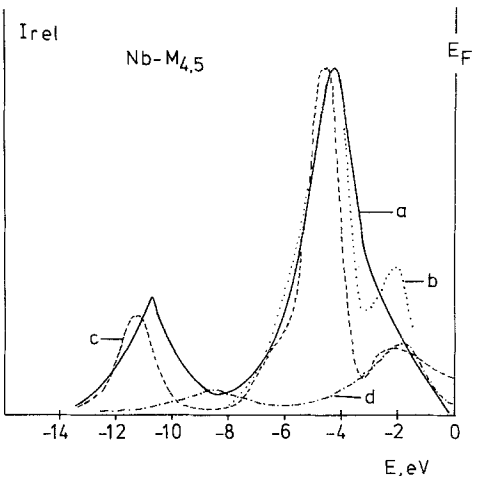

Fig. 5. The Nb-$M_{4,5}$ emission spectrum for NbC in the energy range of M_5-spectrum: (a) experimental M_5 spectrum [16], (b) experimental $M_{4,5}$ spectrum [17] shifted such that the highest peak in (b) coincides with corresponding peak of (a), (c) theoretical M_5 spectrum, (d) theoretical M_4 spectrum

In Fig. 6 the experimental Nb-L_3 spectrum is compared with the theoretically calculated L_3 and L_2 spectra (Table 2). Since the $2p^{1/2}$ and $2p^{3/2}$ core levels differ already by 3.522 a.u. in energy the L_3 and L_2 spectra are well separated. For this reason the theoretical L_2 spectrum is displayed in the same relative energy and relative intensity scale as the L_3 spectrum. In all cases investigated the separation of bands predicted by the theoretical spectra is in good agreement with the experimental data. The relative theoretical intensities agree well with experiment.

4. Conclusion

The application of relativistic transition probabilities is of crucial importance for emission spectra of metals or compounds with heavy constituents ($Z \gtrsim 50$) because here the relativistic effects in the valence region are important [11]. For $Z \lesssim 50$, the relativistic approach is useful for all cases where the separation of

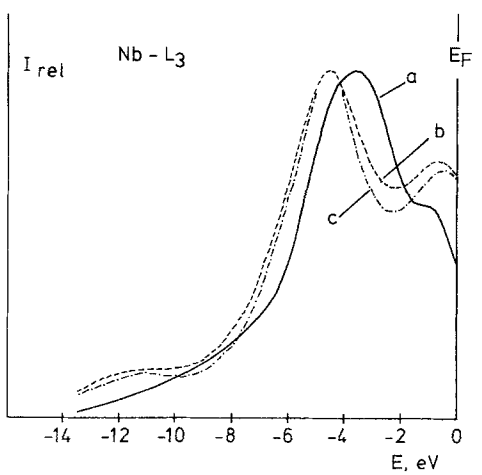

Fig. 6. The Nb-L_3 emission spectrum in NbC: (a) experimental L_3 spectrum [17], (b) theoretical L_3 spectrum, (c) theoretical L_2 spectrum displayed in the same relative energy and intensity scale as the L_3 spectrum

corresponding core levels is small, such as for the Nb-*M* spectrum. In this case non-relativistic local density of states functions can be used. It should be noted, however, that neither the relativistic approach nor the non-relativistic method can account for relaxation effects or secondary processes caused by many-body effects.

Acknowledgement. The authors are grateful to Professors A. Neckel and P. Schuster for their continuous interest in this work. All computations were performed using the facilities of the Technical University of Vienna Computing Centre.

References

1. Neckel, A., Schwarz, K., Eibler, R., Rastl, P., Weinberger, P.: Mikrochim. Acta Suppl. **6**, 257 (1975)
2. Weinberger, P.: Theoret. Chim. Acta (Berl.) **42**, 169 (1976)
3. Rosner, H. R., Bhalla, C. P.: Z. Phys. **231**, 347 (1970)
4. Rose, M. E.: Multipole fields. New York: Wiley 1955
5. Yang, Y., Rabii, S.: Phys. Rev. **A12**, 362 (1975)
6. Rosicky, F., Weinberger, P., Mark, F.: J. Phys. B: Atom. Mol. Phys. **9**, 2971 (1976)
7. Onodera, Y., Okazaki, M.: J. Phys. Soc. Japan **21**, 1273 (1966)
8. Takada, S.: Progr. Theoret. Phys. **36**, 224 (1966)
9. Soven, P.: Phys. Rev. **137A**, 1706 (1965)
10. Loucks, T. L.: Phys. Rev. **139A**, 1333 (1965)
11. Weinberger, P.: Ber. Bunsenges. Phys. Chem. **81**, 804 (1977)
12. Neckel, A., Rastl, P., Eibler, R., Weinberger, P., Schwarz, K.: J. Phys. C: Solid State Phys. **9**, 579 (1976)
13. Schwarz, K.: J. Phys. C: Solid State Phys. **10**, 195 (1977)
14. Fischer, D. W.: J. Appl. Phys. **40**, 4151 (1969)
15. Schwarz, K., Neckel, A.: Ber. Bunsenges. Phys. Chem. **79**, 1071 (1975)
16. Nemoshalenko, V. V., Krivitskii, V. P., Nesenjuk, A. P., Nikolajev, L. I., Shpak, A. P.: J. Phys. Chem. Solids **36**, 277 (1975)
17. Ramqvist, L., Hamrin, K., Johannson, G., Gelius, U., Nordling, C.: J. Phys. Solids **31**, 2669 (1970)
18. Blochin, M. A.: Methoden der Röntgenspektralanalyse. Leipzig: B. G. Teubner Verlagsgesellschaft 1963

Received January 20, 1978